Jour. Geol. Soc. India (2022) 98:260-270
https://doi.org/10.1007/s12594-022-1966-5

ORIGINAL ARTICLE

The Effect of Discontinuity Orientation and Thickness of the Weathered Layer on the Stability of Lesser Himalayan Rock Slope

Arunava Ray[1,*], Rajesh Rai[1] and T. N. Singh[2]

[1]Department of Mining Engineering, IIT (BHU), Varanasi – 221 005, India
[2]Department of Earth Sciences, IIT Bombay, Powai, Mumbai – 400 076, India
E-mail: *arunavar.rs.min16@iitbhu.ac.in*; rajeshrai.min@iitbhu.ac.in; tnsingh@iitb.ac.in*

Received: 11 May 2020 / Revised form Accepted: 17 July 2021
© 2022 Geological Society of India, Bengaluru, India

ABSTRACT

The effect of discontinuity orientations and thickness of the weathered layer in the stability of jointed phyllite rock slopes of the Lesser Himalayan region was examined in this study. Numerical simulation was performed using the Rocscience RS2 V9 finite element software package. The performance of the slope was assessed for varying slope height, slope angle, weathered layer thickness, and orientation of the main joint and the cross joint set. The results indicate that the stability of rock slope depends on the relative orientation and distribution of the contained joint sets and the thickness of the weathered layer. Based on numerical simulation, the order of percentage reduction of a factor of safety (FOS) for the critical combination of joint sets has been identified. It was deduced that while keeping all the parameters constant, the effect of cross joint orientations is prominent in the case of shallow weathered layer and reduces as the thickness of the weathered layer increases. The effect of main joint orientations is prominent in the case of a deep weathered layer and reduces as the thickness of the weathered layer decreases. Analysis of variance (ANOVA) of the obtained result indicates that all the independent variables (slope height, slope angle, weathered layer thickness, main joint set, and cross joint set) are significantly predicting the dependent variable (FOS of rock slope) and the reducing order of significance is weathered layer thickness, slope angle, main joint orientation, slope height, and cross joint orientation.

INTRODUCTION

The extreme sub-tropical climatic condition of the Himalayas has influenced physical and chemical weathering resulting in the formation of highly fractured rock on the surface (Sarkar et al. 2016; Singh et al. 2015). Rock slope instabilities constitute a significant hazard for human settlements, often causing property damages, economic losses, repair and maintenance costs, and in extreme cases injuries or fatalities (Latha and Garaga 2010b; Sarkar et al. 2016; Siddque and Pradhan 2018; Umrao et al. 2011). Large rockslides influenced by structural features such as bedding planes, faults, and joints are often frequent in this area (Anbarasu et al. 2009; Latha and Garaga 2010a; Pain et al. 2014).

Though the strength of the rock plays a critical role in the rock slope stability, geological discontinuities significantly influence the stability of slopes in jointed rock masses (Ghosh et al. 2010; Hencher 1987; Kim et al. 2007; Latha and Garaga 2010a). Discontinuities are weak planes within rock mass, including joints, weak bedding planes, weak zones and faults that reduce rock strength (ISRM 1978). The influence of both weathering and large-scale discontinuities on the stability of rock slopes were investigated using 3D scaled physical models by Bachmann et al. (2004). Barton et al. (1974) pointed out that discontinuities within the rock mass have minimum tensile strength; thus, every single discontinuity has reducing effects on the strength of rock mass, so the chances of rock failures become prominent. The behaviour of rock slopes is the manifestation of the type and frequency of discontinuities present in the rock mass (Einstein et al. 1983; Li et al. 2019). Studies by Hencher (1987), Pal et al. (2012) and Singh et al. (2015) concluded that a single joint seldom governs the stability of slopes rather than a set of discontinuities which as a whole constitutes the governing factor responsible for failure.

The behaviour of rock slopes depends kinematically on the spatial distribution and orientation of the discontinuities (Kothyari et al. 2012; Lie and Hack 2015). The effect of orientation of discontinuities with respect to slope face was studied in detail by Lie and Hack (2015), who concluded that the influence of internal discontinuities on the shear strength is more pronounced when the orientation of the former changes from dipping "with" to dipping "against" the slope face. Starzec and Andersson (2002); Brideau et al. (2009) and Fereidooni (2018), in their study, concluded that the rock slope is sensitive to major geological discontinuities such as folds, fractured or weak zone, faults, and strata interface than any other factors affecting its stability. Structural features control the rock mass behaviour either by stabilisation or destabilisation, depending on the persistence and orientation of the discontinuities (Shang et al. 2018; Zhang and Einstein 2000).

The stability analysis of rock slopes has always been a challenging task for civil and mining engineers because of the intricate jointing pattern of the inherent discontinuities, resulting in different types of slope failures varying from translational to complex multi-mechanism failure (Ghosh et al. 2014; Lie and Hack 2015; Pain et al. 2014; Stead and Wolter 2015). The plane failure is a particular case of rock failure, in which the discontinuity is in the form of joint planes inclined to the horizontal slope face (Shukla and Hossain 2011). Due to the involvement of only a single surface, 2D analysis can be performed

utilising the concepts of a block resting on an inclined plane at a limiting equilibrium. Plane failure is beneficial for depicting the vulnerability of the slope towards failure owing to the changes in discontinuity orientations with respect to the slope surface (Johari and Lari 2017).

This paper outlines the critical role of the weathered layer and the orientations of structural discontinuities in deciding rock slope behaviour. Numerical simulations have been performed by utilising field and laboratory investigations data coupled with a detailed literature study to understand the effect of orientations of different sets of joint on the overall stability of the slope and to identify the most critical discontinuities orientation for a given rock slope profile. Probabilistic analysis has been carried out to simulate the highly uncertain geo-material of the study area. Uncertainty in material occurrence and properties is considered one of the significant factors affecting the accuracy of stability analysis. Though its effect cannot be eliminated but can be minimised to a large extent using probabilistic analysis. ANOVA has also been performed to determine the significance and mathematical relationship among a set of input parameters- joint orientations and slope parameters, for predicting the outcome FoS from the developed model.

AREA OF STUDY

Himalayan orogeny is the outcome of the collision of Indian and Eurasian plates. This region is extensively deformed due to isostatic adjustment of tectonic plates resulting in the formation of three major thrusts or fault zones: The Main Central Thrust (MCT), The Main Boundary Thrust (MBT), and The Main Frontal Thrust (MFT) (Israil and Pachauri 2003; Kothyari et al. 2012; Singh et al. 2014). The MCT, a mylonitic zone on the scale of kilometres, divides the Greater Himalayas from the Lesser Himalayas. The MBT divides the Lesser Himalayas from the Shiwaliks, while the MFT is the outer limit of the Himalayas dividing the Shiwaliks from the Tarai planes (Bartarya and Valdiya 1989; Kothyari et al. 2012; Siddique et al. 2017). The rocks that occur in the Himalayas vary from soft sedimentary rocks in the Shiwaliks to highly weathered metamorphic rocks in Greater Himalayas. The rock mass is extensively folded, cleaved, and jointed (Sarkar et al. 2016). Moderate to steep slopes are the key geomorphological features of the Himalaya (Kumar et al. 2017). The hill slopes lie at an average angle of 35^0, steepening locally to 50^0 and sometimes can be of nearly vertical rock slope (Bartarya and Valdiya 1989; Mehrotra et al. 1996). The Himalayan hill slopes are well known for instabilities due to their geomorphology, ongoing neotectonics activity, heavy and sustained rainfall at lower elevations coupled with snowfall at the higher elevations. Increasing anthropogenic activities in recent years appear to be an additional factor for instability of slopes in this region (Kumar and Anbalagan 2016; Kumar et al. 2017).

This study focuses on the stability analysis of rock slopes in the Lesser Himalayan region bounded by the MCT and MBT. The rocks which frequently occurs in Lesser Himalaya include phyllites, limestones, and gneiss, which are intensely fractured, jointed and sheared, making the rocks highly susceptible to sliding (Gerrard 1994; Regmi et al. 2014). The rugged nature of the rocky slopes in this area results in average inclination angle ranging between 45° to 75° (Bartarya and Valdiya 1989; Mehrotra et al. 1996; Ray et al. 2019). Field investigations and structural mapping of these rocks by Gerrard (1994), Regmi et al. (2014) and Brideau et al. (2009) demonstrated deep weathering leading to an increase in microfissuration and discontinuities, thereby reducing the overall strength of bedrock. A detailed study by Gerrard (1994) and Regmi et al. (2014) revealed that the phyllites are most vulnerable to rock disintegration due to weathering and shearing, followed by shales, schists, poorly cemented sandstones, gneiss, granites, and quartzite.

A typical problem frequently faced in this region is the inherent heterogeneity of the slope materials (Siddque and Pradhan 2018). Uncertainties in mechanical properties of lithologies arise due to geological anomalies, variable environmental conditions, inherent anisotropy in geomaterial properties, and various anthropogenic activities (Jiang et al. 2015; Kumar and Anbalagan 2016; Park et al. 2005). For assessing the behaviour of a slope, deterministic factor of safety (FOS) calculation has been traditionally used. The prime demerit in the application of deterministic FOS lies in the fact that it uses a particular value for all material parameters ignoring the fact that lithologies by nature are fundamentally heterogeneous, and so-called homogenous materials also display a certain amount of inconsistent in their physio-mechanical properties (Ersöz and Topal 2018; Pathak and Nilsen 2004; Ray et al. 2019). Almost all the parameters in rock mechanics, which includes the loading conditions, the rock strength properties, and joint set characteristics, are statistical (Carter and Lajtai 1992). Extensive literature studies also reveal that the slopes designed based on the deterministic analysis sometimes fails even in cases where the calculated FOS more than unity. Therefore, the presence and significance of uncertainties in slope stability analysis have long been appreciated. Consequently, the probabilistic approach is gaining importance over the years since they can effectively deal with the uncertainty and incorporate it into the analysis (Johari and Lari 2017). The probabilistic method provides a statistical distribution function of each geomechanical parameter that stipulates the uncertainties involved in the geomaterial (El-Ramly et al. 2005; Pathak et al. 2006).

METHODOLOGY

In any analysis involving rock slope, the primary step is always the gathering of discontinuity data from the field. Numerous investigations performed during field study include lithological studies of the physical properties of the rocks, scanline survey for determinations of orientation and distribution of discontinuities and the joint filling materials. Various equipment that has been used in field surveys include Measurement Tape (15m), a Geological Hammer (Estwing E3-24BLC Rock Picks (Chisel Head)), Brunton Compass (PIE BTC1), Digital Rock Schmid Hammer (Proceq, Swiss Make-Type N), and Core Extractor.

A large number of discontinuity orientations and geometries were identified in the field, and their random properties were evaluated. Four sites were selected in Lesser Himalaya, having phyllite rock outcrop. Unconfined compressive strength (UCS) values obtained from Schmidt hardness values are cost-effective, quick, non-destructive, and considers the variations in strength characteristics that are being posed due to discontinuities and several geological disparities within the rock mass (ASTM D5873; Deere and Miller 1966; Siddque and Pradhan 2018). Hence, as per the recommendations of the International Society for Rock Mechanics (ISRM) and Hudson (2007), UCS and density of the rock mass have been determined by using Schmidt hardness values. Based on roughness and Schmidt hammer values of the discontinuities, the friction angles between discontinuities were found by Barton and Bandis (1990) equation. The summary of structural features identified at the sites is given in Table 1. Representative samples were also collected in the form of rock core from the sites, and the material and mechanical properties of the rock mass were obtained through laboratory testing (as per ASTM D7012; ASTM E132 – 04) are given in Table 2.

The interpretation of the field data is not necessarily a simple process. For instance, joint orientation is subject to error and bias. However, the bias in orientation and other parameters, such as joint spacing, trace length, and persistence, can be treated quantitatively to correct errors in measurement by using the probabilistic method (El-Ramly et al. 2005; Pathak and Nilsen 2004; Starzec and Andersson 2002). One of the necessary conditions for using probabilistic analysis is the availability of a sufficient amount of data in order to develop the

Table 1. Field observation of discontinuity parameters

Location	No. of Joints	Joint Dip Amount (deg)	Joint Spacing (m)	Joint Persistence (m)	Infilling	Schmid Hammer Rebound Number (R)
Pipalkoti, Uttarakhand	3	15 – 60	0.06 – 1.0	0.2 – 1.2	Clay	20
Rampur, (near Augustmuni) Uttarakhand	2	10 – 85	0.01 - 0.05	0.1 - 1.5	Clay	15
Sataun, Sirmur district, Himachal Pradesh	2	35 – 75	0.06 - 0.15	0.2 – 1.0	Sand	24
NH-119, Srinagar, Uttarakhand	3	15 – 80	0.05 - 0.2	0.3 – 1.0	Clay	28

Table 2. Laboratory testing results

Location	Unit Weight (MN/m^3)	Young Modulus (GPa)	Poisson's Ratio	UCS (Mpa) (From R)	C (MPa)	Φ (deg)
Pipalkoti, Uttarakhand	0.026	12.0	0.25	16	0.310	36.5
Rampur, (near Augustmuni) Uttarakhand	0.027	9.5	0.25	08	0.280	32.5
Sataun, Sirmur district, Himachal Pradesh	0.027	16.0	0.20	27	0.475	42.0
NH-119, Srinagar, Uttarakhand	0.026	22.5	0.22	33	0.610	41.5

probability density function (PDF) for each variable. To augment the quantity, a detailed literature survey has also been made, and a compiled engineering property is summarised in Table 3 and Table 4. The empirical relationship proposed by Abdaqadir and Alshkane (2018) was used for obtaining the missing data of Table 4 by using the respective UCS values. Once sufficient data is generated through field experiments, laboratory testing and literature survey, the PDF was identified for each parameter and stability analyses were proceeded by using probabilistic techniques augmented by Monte Carlo simulations (Carter and Lajtai 1992; Einstein et al. 1983; Park et al. 2005).

Utilising the data from Table 1-4, models were prepared by varying the slope height, slope angle, depth of weathered layer and orientations of joint sets. The height of the slope was varied from 100m to 500m with an interval of 100m. The study by Ersöz and Topal (2018) and Ray et al. (2019) combined with field visits revealed that most of the rock slope (slope having minimal soil cover or completely devoid of soil cover) in the Himalayas has a slope angle of greater than 45°-50°. The slope angle used for simulation was varied from 45° to 75° with an interval of 15°. The presence of a humid tropical climate, along with the occurrence of monsoonal rain, has resulted in intense weathering of the bedrock in the study region. An essential behaviour of weathering in a tropical climate is that it reduced with depth; thus, the weathered layer (top layer in modelling) is divided into two equal parts resembling a highly fractured top layer and a moderately fractured bottom layer (Little 1969). The thickness of the entire weathered layer varied from 4m to 20m with an interval of 4m. For the weathered layer, a cross-joint (two oblique discontinuity sets, which is representative of most joint geometries observed in the field) has been used, having four mean possible adverse discontinuity orientations for each discontinuity set (Table 5). The discontinuity spacing was modelled by using lognormal distribution as proposed by Park et al. (2005). For replicating actual site behaviour, the moderately weathered bottom layer has been modelled with half the discontinuity density of that of the highly weathered top layer. The cross joints in the weathered layer have been modelled, assuming a mean persistence of 0.8. For achieving a simple parametric description of the discontinuity geometry, discontinuities are assumed to be planar. Although

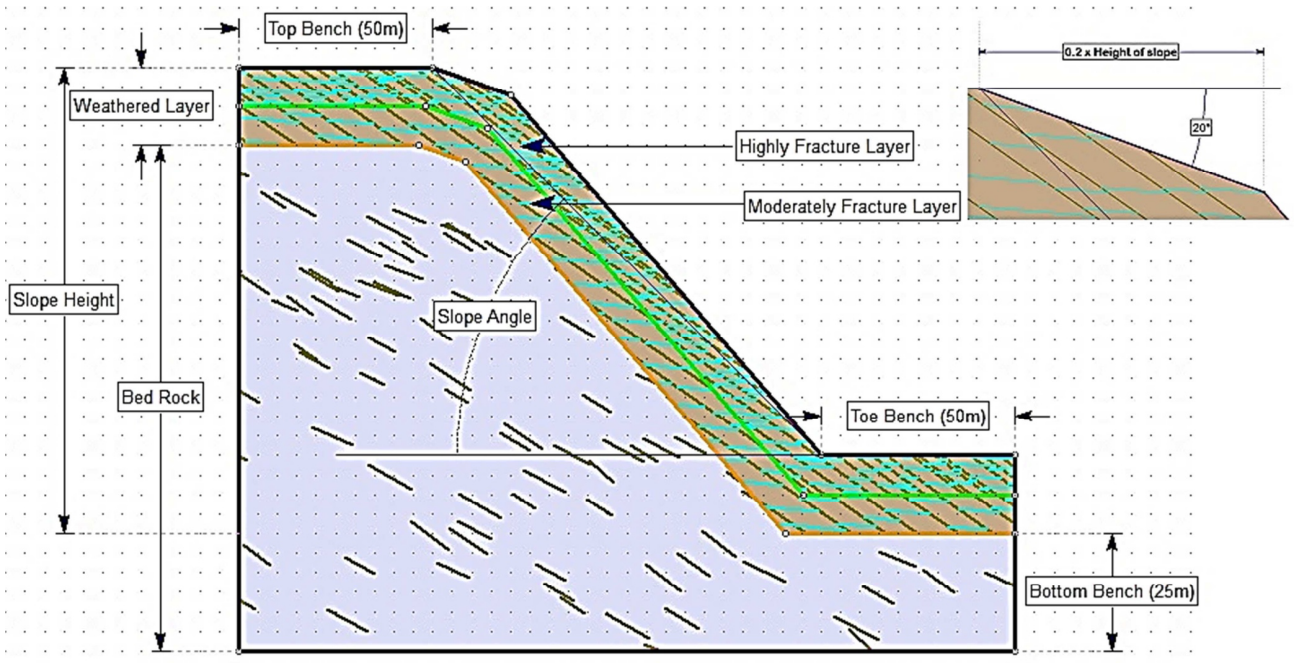

Fig.1. Basic slope model used for numerical simulation

Table 3. Compiled literature data of discontinuity properties in the study area

Source	Location	No. of Joint	Joint Dip Amount (deg)	Joint Spacing (m)	Joint Persistence (m)	Joint roughness	Joint infilling
Umrao et al. (2011)	Rudraprayag District, Uttarakhand	3 - 5	45 - 81	0.06	10 - 20	Smooth	Hard filling
Mahanta et al. (2016)	Kullu District, Himachal Pradesh	2 - 4	19 - 80	-	-	-	-
Gupta and Tandon (2015)	Upper Alaknanda Valley, Uttarakhand	3 - 5	10 - 88	0.06 - 2	-	Slickensides to Soft gouge	-
Chaurasia et al. (2017)	Gangadarshan, Pauri, Gharwal, Uttarakhand	1 - 3	20 - 80	0.06 - 0.72	0.1 - 1.5	Smooth to Rough	Clean joint to clay
Pathak and Nilsen (2004)	Kali Gandaki hydropower project, Nepal	3	51 - 58	0.01 - 0.4	-	Planar to undulating	-
Siddique et al. (2017)	NH 58, Uttarakhand	2 - 3	-	0.2 - 0.6	3 - 20	Slightly rough	Clean joint to soft
(Singh et al. 2014; Singh et al. 2017)	Rudraprayag District, Uttarakhand	2	-	-	-	-	-
Pradhan et al. (2018)	Rudraprayag District, Uttarakhand	3	-	-	-	-	-
Singh et al. (2015)	Luhri, Himachal Pradesh	3	70 - 80	0.2 - 1.5	0.2 - 2	Slight smooth	Sand to clay

Table 4. Rock mass data compiled from the literature

Source	Location	UCS (MPa)	Young Modulus (GPa)	Friction angle (deg)	C (MPa)	Poisson Ratio	Unit Weight (MN/m^3)
Umrao et al. (2011)	Rudraprayag District, Uttarakhand	28	-	-	-	-	-
Mahanta et al. (2016)	Kullu District, Himachal Pradesh	58 - 94	6 - 11	37 - 50	0.233 - 0.356	0.25	0.026
Gupta and Tandon (2015)	Upper Alaknanda Valley, Uttarakhand	4 - 40	-	-	-	-	0.027
Chaurasia et al. (2017)	Gangadarshan, Pauri, Gharwal, Uttarakhand	13 - 48	-	-	-	-	-
Pathak and Nilsen (2004)	Kali Gandaki hydropower project, Nepal	17	-	32 - 58	-	-	-
Siddique et al. (2017)	NH 58, Uttarakhand	15 - 23	-	-	-	-	-
Singh et al. (2014); Singh et al. (2017)	Rudraprayag District, Uttarakhand	28	12	24	0.046	0.18	0.027
Pradhan et al. (2018)	Rudraprayag District, Uttarakhand	41	25	40	9-13.5	0.26	0.029
Singh et al. (2015)	Luhri, Himachal Pradesh	38 - 78	25	36 - 40	6	-	-

Table 5. Cross Joint orientations and persistence

Joint Set 1 mean Dip angle	5°	25°	45°	65°
Joint Set 2 mean Dip angle	-10°	10°	30°	50°
Standard Deviation of Dip angle for both the Joint Sets	0.5°	0.5°	0.5°	0.5°
Mean Persistence of both the joint set	0.8	0.8	0.8	0.8
Standard Deviation of persistence for both the Joint Sets	0.05	0.05	0.05	0.05

discontinuities can be curved or wavy in some cases, this curvature is often negligible (Zhang and Einstein 2000).

Based on all the above-discussed conditions,1200 numerical models were prepared by incorporating five variations in slope height, three variations in slope angle, five variations in weathered layer thickness, and four variations of each cross joint set. In all the models, 50m bench width is maintained at both the crest and the toe of the slope. A depth of 25m is maintained below the toe in all slopes (Fig. 1). As proposed by Einstein et al. (1983), Veneziano joint network model has been selected for the bedrock, with a mean joint length of 10m and a mean persistence of 0.8. The discontinuities in the bedrock are modelled using the exponential distribution for joint length and lognormal distribution for joint spacing, as suggested by Park et al. (2005). Simulations have been performed using Rocscience RS2 V9.0 (https://www.rocscience.com), a finite element package for analysing stability and deformation based on the shear strength reduction (SSR) technique. Singh et al. (2017) studied the effect of utilising 2D and 3D in stability analysis concluded that in uniform rock materials, the FOS in the 3D analysis is not influenced by slope width. The 3D analysis will be better suited either in lateral variation in rock mass properties or the presence of weak layer/material(s) in slopes. Since the present work focuses on the stability aspect of rock slope composed of phyllite, a 2D FEM analysis has been used. Based on the developed PDF of each variable, the statistical parameters such as mean, standard deviation, relative minimum, and relative maximum were developed and tabulated in Table 6.

After completing the numerical simulation, a correlation matrix was developed to investigate the relationship between multiple independent variables and between the independent variables and the output (FOS in this case). Correlation is a statistical technique used to depict whether and how strongly pairs of variables are related. ANOVA was also conducted to evaluate the strength/significance of slope physical parameters like slope height, slope inclination, depth of weathered layer, main joint set (MJS) orientation, and cross joint set (CJS) orientation on predicting the stability (FOS) of the slope. Thus, ANOVA helps to understand how the dependent variable will behave when there is a change in the independent variables. It can also be utilised to predict trends and future values. Unlike regression, ANOVA does not presume linear relationships; thus, it manages interaction effects automatically. It is not a test of difference in variances but

Table 6 Statistical parameters used for numerical simulation

S. No.	Property	Distribution	Mean	Standard Deviation	Relative Minimum	Relative Maximum
	Statistical Properties of Weathered Layer Rock Mass					
1	Young's Modulus (GPa)	Normal	15.5	5.78	9.72	21.28
2	Tensile Strength (MPa)	Normal	0.308	0.02	0.248	0.368
3	Friction Angle (deg)	Normal	42.14	5.44	25.82	58.46
4	Cohesion (MPa)	Normal	0.744	0.04	0.624	0.864
	Statistical Properties of Joint set in Weathered Layer					
1	Normal Stiffness (GPa/m)	Normal	18.0	4.5	13.5	22.5
2	Shear Stiffness (GPa/m)	Normal	2.5	0.8	1.7	3.3
3	Cohesion (MPa)	Normal	0.1275	0.073	0.0515	0.2005
4	Friction Angle (deg)	Normal	34.53	1.12	31.17	37.89
	Statistical Properties of Jointed layer between Weathered Layer and Bed Rock					
1	Cohesion (MPa)	Normal	0.4	0.01	0.375	0.435
2	Friction Angle (deg)	Normal	39.625	2	34	46
	Statistical Properties of Bed Rock					
1	Young's Modulus (GPa)	Normal	39.5	2.95	36.55	42.45
2	Tensile Strength (MPa)	Normal	2.484	0.38	1.344	3.624
3	Friction Angle (deg)	Normal	35.95	4.0	23.95	47.95
4	Cohesion (MPa)	Normal	9.35	0.62	7.49	11.21

rather an assumption of the relative homogeneity of variances. Thus, the key assumptions in ANOVA analysis are that the groups formed by the independent variables are relatively equal in size, and the independent variables must not strongly correlate. Like regression, ANOVA is a parametric procedure that assumes multivariate normality (Kim et al. 2007).

RESULTS AND DISCUSSION

After performing the required number of numerical simulations, the FOS values for every model were obtained. For the present work, the notation given in Table 7 has been used for depicting the combination of the MJS and CJS orientations.

The effect of discontinuity orientation and the thickness of the overall weathered layer for a slope having an inclination of 45° is shown in Fig. 2. The result indicates a continuous decrease in FOS with an increase in depth of the weathered layer for a constant slope height and given joint orientations. The graphs indicated a significant reduction in FOS for joint set orientations of 9, 10, 11, 12, i.e., when the MJS has a dip angle same as that of slope inclination for different slope height and weathered layer thickness. There is also a slight reduction in FOS for joint set orientation of 3, 4, 8, 15, and 16, which have the CJS dip in between $\pm 15^0$ of slope inclination. The more the deviation of MJS dip from the slope inclination, the more stable is the slope, provided that the cross CJS dip is also deviating much from the slope angle. For this particular case, the safest joint orientation correspondence to the MJS orientation of 5° and CJS orientation of 10° for all heights and thickness of weathered layer. The lowest FOS of around 1.4 was obtained for a slope of 500m height and 20m thick weathered layer having MJS dip of 45° and CJS dip of 10°. The maximum FOS was obtained for the 300m height slope having 4m thick weathered layer and MJS dip of 5° and CJS dip of 10°.

In the case of the slope with an inclination of 60°, the effect of discontinuity orientation and the thickness of the overall weathered layer is shown in Fig. 3. The same pattern of continuous decrease in FOS with an increase in depth of the weathered layer for a constant slope height and given joint orientations as in 45^0 slopes is also observed. The significant reduction in FOS occurs for joint set orientations of 13, 14, 15, 16, i.e., for the joint combinations where the MJS has a dip in between $\pm 15^0$ of slope inclination. The graph also shows a slight reduction in FOS around joint combinations 4 and 8, which may be attributed to the fact that CJS dip in between $\pm 15^0$ of slope inclination. In this case, also, the slope is more stable when the deviation of the MJS from the slope inclination is more provided the CJS is also deviating much from the slope angle. The lowest value of FOS, in this case, is around 0.94 obtained for a slope of 500m height and 20m thick weathered layer having an MJS dip of 65^0 and CJS dip of 10^0. The maximum FOS was obtained for the 400m height slope having 4m thick weathered layer and MJS dip of 5^0 and CJS dip of 10^0.

The effect of discontinuity orientation and the thickness of the overall weathered for slope inclining 75° is shown in Fig.4. The same pattern of continuous decrease in FOS with an increase in depth of the weathered layer for a constant slope height and given joint orientations as in 45° and 60° slopes is also observed. The minimum FOS occurs for joint set orientations of 13, 14, 15, 16, i.e., for the joint combinations where the main MJS has a dip in between ±15° of slope inclination. A close look into Fig. 4 shows almost constant FOS for different joint combinations excepts for joint set orientations of 13, 14, 15, and 16, which may be attributed to the fact that the CJS orientations taken for simulation do not fall in between ±15° of slope inclination thus only the effect of MJS is prominent in FOS for the slope. The lowest value of FOS is around 0.98 which is from a slope of 500m height and 20m thick weathered layer having MJS dip of 65° and CJS dip of 10°. The maximum FOS was obtained for the 500m height slope having 4m thick weathered layer and MJS of 5° and CJS dip of 30°.

Table 7 Notations used for joint combinations

Mean MJS dip	5°	5°	5°	5°	25°	25°	25°	25°	45°	45°	45°	45°	65°	65°	65°	65°
Mean CJS dip	-10°	10°	30°	50°	-10°	10°	30°	50°	-10°	10°	30°	50°	-10°	10°	30°	50°
Denoted as	1	2	3	4	5	6	7	8	9	10	11	12	13	14	15	16

From the results, it can be concluded that there is a drastic reduction in FOS as the thickness of the weathered layer increases above 4m for all slope heights and angles. As the thickness of the weathered layer increases by more than 10m, there is significantly less variation in FOS for every slope height and angles. As the slope changes from moderate to steep, the variation of FOS for any particular weathered layer thickness reduces, and the slope behaves in an almost similar manner for different joint set orientations except for the case when the MJS and CJS dip in between ±15° of slope inclination. Significant reduction in FOS is observed when the MJS dip in between ±15° of slope inclination, and minor reduction occurred when CJS dip in between ±15° of slope inclination. Analysis of results indicated there are around 46 cases where FOS is less than one, and out of this nearly 84% are cases where the MJS dip occurs in between ±15° the slope inclination and rest are due to CJS dip in between ±15° the slope inclination. Thus, it could be implied that the MJS governs the overall stability of the rock slope. In term of discontinuity orientations, the FOS of any rock slope having a combination of two joint sets decreases in the order of both the joint set orientation differ more than ±15° of the slope inclination; the MJS orientation differs more than ±15° of the slope inclination but the CJS orientation falls in between ±15° of the slope inclination; the CJS orientation differs more than ±15° of the slope inclination but the MJS orientation falls in between ±15° of the slope inclination, and least in the case when both the joint set orientation falls in between ±15° of the slope inclination. This order is appropriate for slope failures within weathered material and not when the failure surface passes through the bedrock layer. Thus, it can be concluded that discontinuity orientations significantly influence the occurrence of a landslide.

For a fine weathered layer thickness of 4m or less, there is an increase in the values of FOS, with an increase in height that can be seen for all the slope angles (Fig. 2, Fig. 3 and Fig. 4). This may be attributed to the fact that as the height of the slope increases, the effect of a weathered layer with 4m or less thickness gets diminishes and only localised rockfall is observed in simulation as well as at sites. However, for slopes possessing a weathered layer of more than 4m thickness, the FOS remains almost constant or decreases with increased slope height. Representative simulation results for different slope heights with the same slope inclination (45°), weathered layer thickness (20m), and the orientation of discontinuities (Joint orientation combination number 11) is shown in Fig.5. It was observed that almost the entire shear strain and deformation vectors are concentrated in the weathered layer for all slope heights. When the slope height is less than 200m, the maximum shear strain and deformation vectors are observed in the top highly weathered layer and up to a certain extent in the bottom moderately weathered layer. However, in both cases, it never reached the entire depth of the weathered layer. With an increase in slope height beyond 200m, the maximum shear strain and deformation vectors are observed in the entire depth of the weathered layer. It was also observed that the majority of the slopes are stable, but few localised failures are observed at the slope face, which may be attributed to the fact that the FOS is derived for the entire model. The strength values of the fresh/undisturbed zones of the slopes are higher than the weathered/disturbed zones. In the case of rock slopes in the study area, there are few cases of deep-seated landslide involving bedrock, but most of the failures are only observed at the surface of the slopes through the joints or degradation of the intact rocks. In continuum codes, damage within a rock slope may be characterised implicitly by considering the change in the number of yielded elements compared to the total number of elements. Analysis of numerical simulation results indicates the maximum yielded elements are around the MJS that is daylighting in the slope face.

The slopes having greater height have maximum horizontal displacements located near the crest, while the slopes with limited

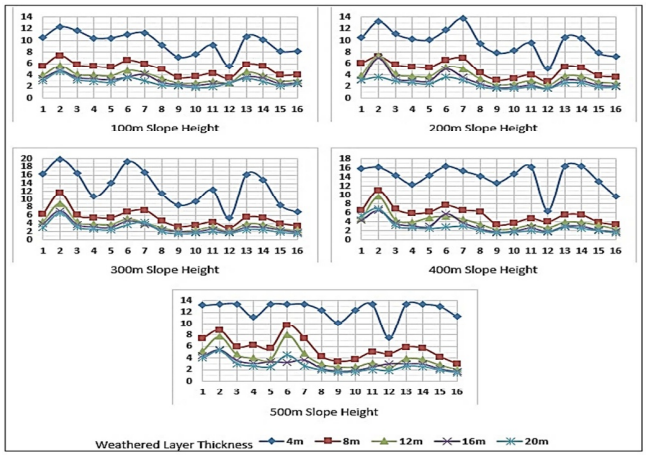

Fig.2. Variation of FOS for different combination of MJS and CJS orientation, slope height and weathered layer thickness for 45° slope inclination (Note: Y-axis represent FOS and X-axis represent Joint Set Orientations)

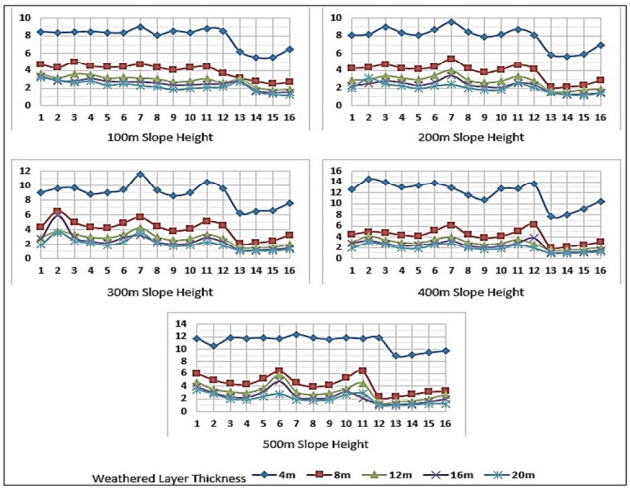

Fig.3. Variation of FOS for different combination of MJS and CJS orientation, slope height and weathered layer thickness for 60° slope inclination (Note: Y-axis represent FOS and X-axis represent Joint Set Orientations)

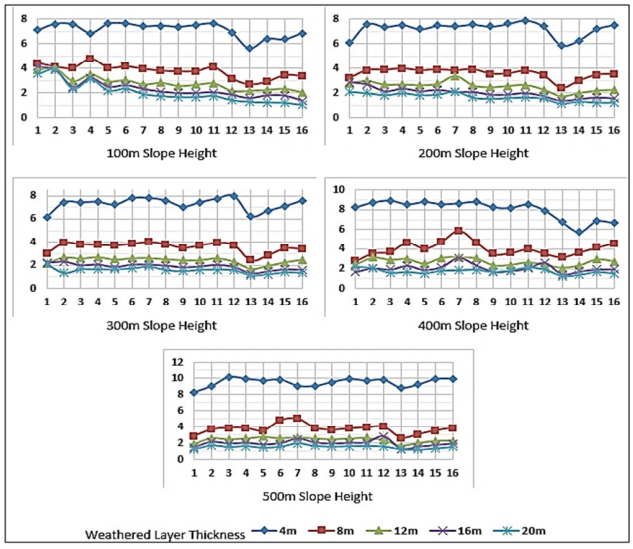

Fig.4. Variation of FOS for different combination of MJS and CJS orientation, slope height and weathered layer thickness for 75° slope inclination (Note: Y-axis represent FOS and X-axis represent Joint Set Orientations)

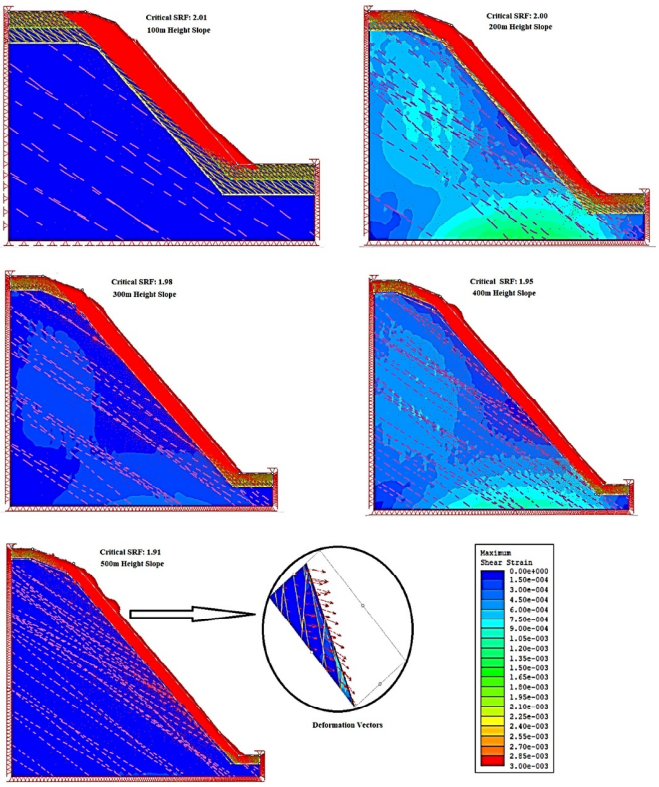

Fig.5. Simulation result depicting the maximum shear strain and deformation vectors for slopes having different heights but with the same slope inclination of 45deg, weathered layer depth of 20m and joint orientation set (Joint Combination Number 11)

height, the maximum horizontal displacement is observed at the toe of the slopes. However, the maximum shear stress and shear strains are observed near the toe of the slope, and maximum vertical displacements are observed near the crest of the slope. It was observed that the slopes with a larger number of plastic points have higher stability, i.e., slopes have undergone permanent deformation (Table 8). The tension cutoff points are located near the crest of the slopes. However, for smaller height slopes, the tension cutoff points are insignificant since strong rocks can sustain themselves even at steep slope geometries, provided the discontinuity orientations are favourable. Rocks which appear to be strong during laboratory tests may be fragile in rock mass due to the development of fractures at the micro/macro scales providing ample weak planes or zones. It could be inferred that the slope instability in the study area is structurally controlled. Field investigation has revealed that the valley dipping joint planes are wide open at some places (more than 3cm even). During rains, percolation of water along these joint planes led to lowering of shear strength of the rock mass, resulting in failure.

The variation of FOS for different slope angles, discontinuity orientations and slope heights for a particular thickness of a weathered

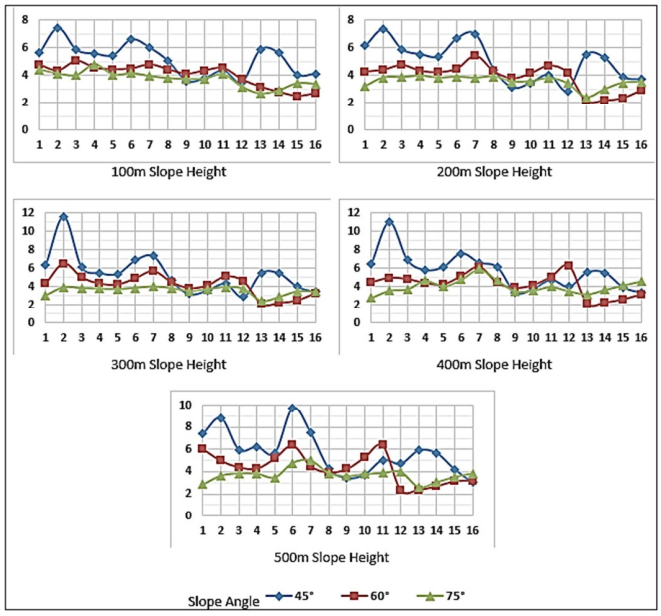

Fig.6. Variation of FOS for different slope height and slope angle for 4m weathered layer thickness (Note: Y-axis represent FOS and X-axis represent Joint Set Orientations)

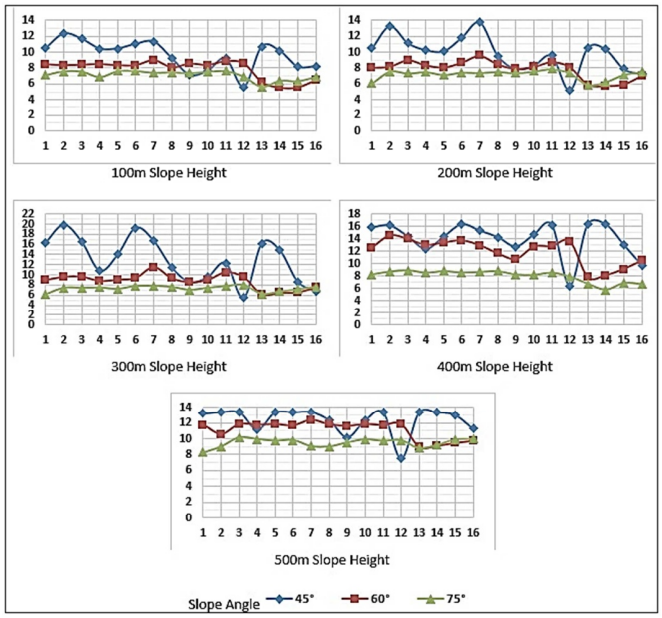

Fig.7. Variation of FOS for different slope height and slope angle for 8m weathered layer thickness (Note: Y-axis represent FOS and X-axis represent Joint Set Orientations)

layer is shown in Fig. 6 to Fig. 10. The variations in FOS are more profound in 45° slopes and reduces as the slope becomes steeper for all thickness of the weathered layer. Also, as the thickness of the

Table 8. Representative number of plastic points observed during numerical simulation for cross joint orientation combination number 5

Slope	8m Weathered Layer						16m Weathered Layer					
Height	45° Slope		60° Slope		75° Slope		45° Slope		60° Slope		75° Slope	
(m)	FOS	Plastic points	FOS	Plastic points	FOS	Plastic points	FOS	Plastic points	FOS	Plastic points	FOS	Plastic points
100	4.91	92	3.97	73	3.64	62	2.84	48	2.47	36	2.25	34
200	4.84	84	3.79	69	3.43	58	2.69	45	2.07	31	1.91	28
300	4.86	87	3.81	72	3.35	55	2.68	47	2.00	32	1.65	25
400	5.52	116	3.82	74	3.64	61	2.66	47	2.25	33	1.69	27
500	5.10	98	4.67	81	3.13	56	3.07	55	2.86	38	1.63	25

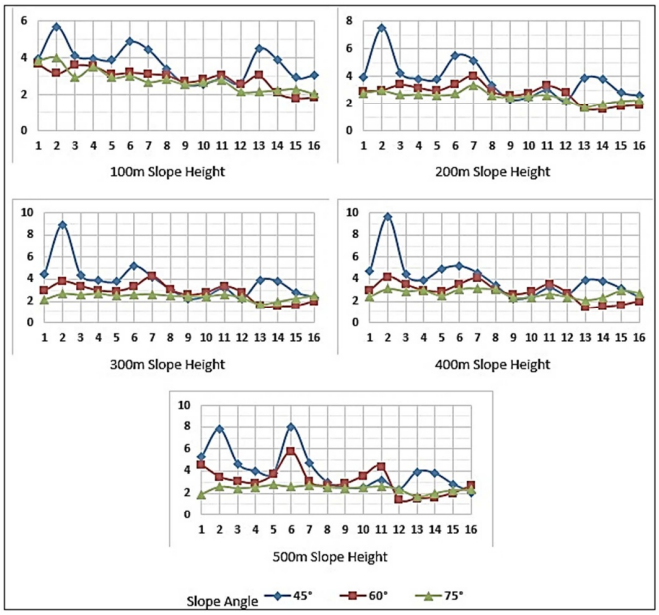

Fig.8. Variation of FOS for different slope height and slope angle for 12m weathered layer thickness (Note: Y-axis represent FOS and X-axis represent Joint Set Orientations)

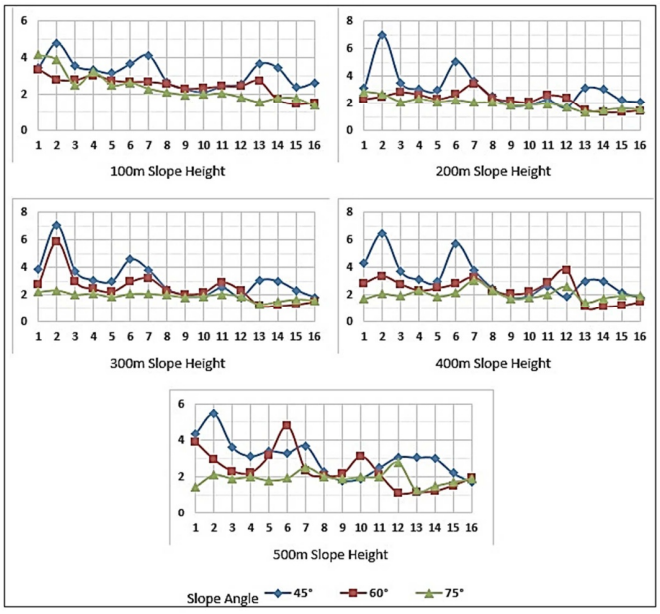

Fig.9. Variation of FOS for different slope height and slope angle for 16m weathered layer thickness (Note: Y-axis represent FOS and X-axis represent Joint Set Orientations)

weathered layer increases, the percentage difference between FOS of 45° and 75° slopes reduces. This implies that as the thickness of the weathered layer increases, the effect of slope inclination on FOS reduces. As the joint orientation inches towards the slope orientation, there is a gradual decrease in the value of FOS.

The effect of variation in the cross joint orientation on the FOS of rock slope while keeping all the parameters constant is shown in Fig.11. In Fig.11a, the slope height is kept constant at 200m, the slope inclination is set at 60°, and the mean MJS dip is 45°. It can be inferred that as the CJS orientation moves closer to the slope inclination angle, the FOS decreases (Fig.11a). The minimum FOS is obtained when the CJS orientation is 50°, i.e., within ±15° of slope inclination angle. Fig.11b shows the variation of FOS for a constant value of the mean

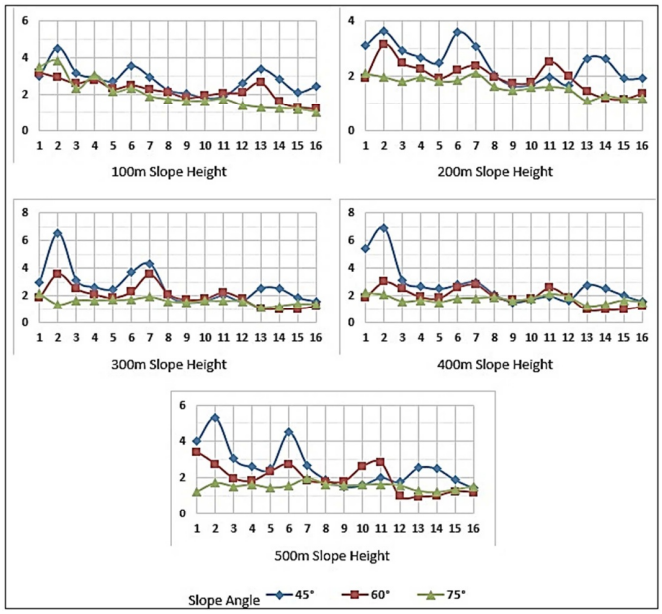

Fig.10. Variation of FOS for different slope height and slope angle for 20m weathered layer thickness (Note: Y-axis represent FOS and X-axis represent Joint Set Orientations)

MJS dip of 45° and varying slope angle and weathered layer thickness. Similarly, the effect of variation in the MJS orientation on the FOS of rock slope while keeping all the parameters constant are shown in Fig.12. Table 9 depicts the average percentage reduction in FOS when the orientation of CJS and MJS is more than ±15° of slope inclination angle to the case when the orientation is in between ±15° of slope inclination angle for different thickness of the weathered layer. Analysis of Table 9 indicates that, when the orientation of CJS changes from safe to critical (from >±15° to in between ±15° of slope inclination angle), keeping all other parameters constant, there is a significant reduction in FOS for the case when the thickness of the weathered layer is small. With the increase in the thickness of the weathered layer, this percentage reduction in FOS reduced. Thus, it can be concluded that the effect of CJS orientations is prominent in the case of shallow weathered layer and reduces as the thickness of the weathered layer increases. This may be attributed to the fact that when the thickness of the weathered layer increases, the effect of CJS in forming a slip surface is hindered by rock bridges and MJS. The effect of MJS orientations in the percentage reduction of FOS as it changes from safe to critical (from $>\pm15^0$ to in between $\pm15^0$ of slope inclination angle), keeping all other parameters constant, is also shown in Table 9. The overall reduction in FOS compared to the CJS is more, but in this case, the percentage reduction increases as the thickness of the weathered layer increases. Thus, it can be concluded that the effect of MJS orientations is prominent in the case of a deep weathered layer and reduces as the thickness of the weathered layer decreases. This

Table 9. Percentage reduction in FOS from safest (>±15° of slope inclination angle) to critical (in between ±15° of slope inclination angle) cross joint orientations

Thickness of weathered layer	% Reduction in FOS	
	Constant MJS (45°) &Varying CJS	Constant CJS (30°) &Varying MJS
4 m	19.15	22.92
8 m	8.95	31.77
12 m	8.55	33.18
16 m	5.83	37.40
20 m	5.30	40.50

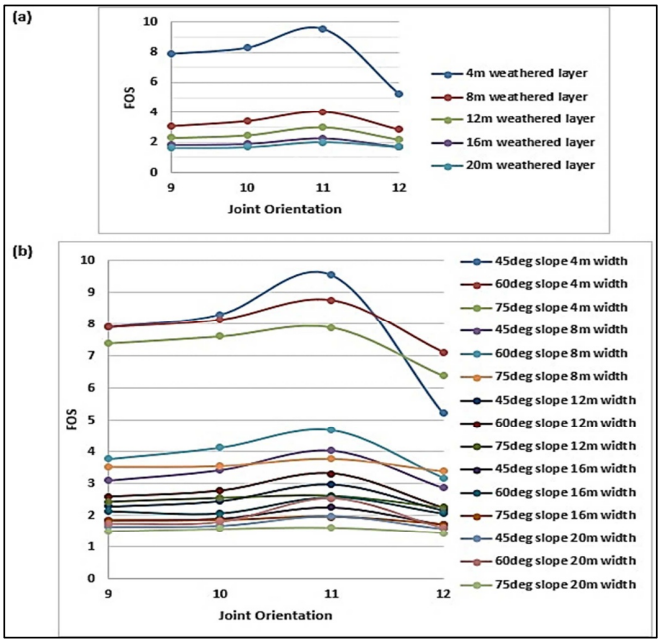

Fig. 11. (a). Shows the variation of FOS with different weathered layer thickness and a varying CJS orientation for a fixed MJS of 45deg and fixed slope height of 200m and slope angle of 60° **(b)** Shows the variation of FOS with different weathered layer thickness, a varying CJS orientation and different slope orientation for a fixed MJS of 45deg and fixed slope height of 200m

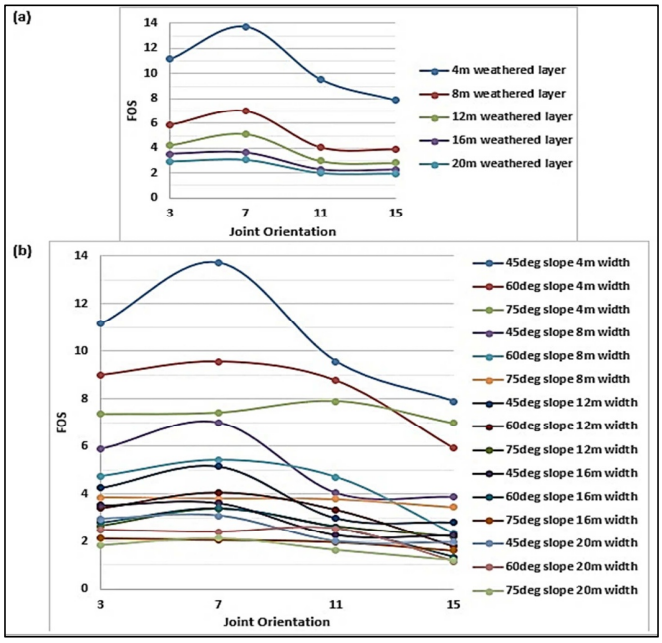

Fig.12. (a) Shows the variation of FOS with different weathered layer thickness and a varying MJS orientation for a fixed CJS of 30° and fixed slope height of 200m and slope angle of 60° **(b)** Shows the variation of FOS with different weathered layer thickness, a varying MJS orientation and different slope orientation for a fixed CJS of 30deg and fixed slope height of 200m

Table 10. Correlation matrix

	Slope Angle	Slope Height	Weathered layer thickness	MJS	CJS	FOS
Slope Angle	1.000					
Slope Height	0.000	1.000				
Weathered layer thickness	0.000	0.000	1.000			
MJS	0.000	0.000	0.000	1.000		
CJS	0.000	0.000	0.000	0.000	1.000	
FOS	-0.227	0.080	-0.751	-0.181	-0.036	1.000

Table 11. ANOVA analysis

Regression Statistics					
Multiple R	0.810259104				
R Square	0.656519816				
Adjusted R Square	0.655081457				
Standard Error	1.885794705				
Observations	1200				
ANOVA					
	df	SS	MS	F	Significance F
Regression	5	8115.948895	1623.189779	456.4366142	5.0285 E-274
Residual	1194	4246.128675	3.556221671		
Total	1199	12362.07757			
		Coefficients	Standard Error	t Stat	P-value
Intercept		14.07392	0.361102	38.9749	0.000000
Slope Angle		-0.05960	0.004445	-13.4077	0.000000
Slope Height		0.00182	0.000385	4.7211	0.000003
Weathered layer thickness		-0.85243	0.019247	-44.2892	0.000000
MJS		-0.51998	0.048691	-10.6792	0.000000
CJS		-0.10389	0.048691	-2.1337	0.033072

may be attributed to the fact that when the thickness of the weathered layer increases, the probability of the MJS forming a slip surface deep inside the weathered layer increases.

ANOVA analysis was also conducted using calculated results from the numerical simulation to analyse the effect of independent variables like slope height, weathered layer thickness, MJS orientation, CJS orientation, and slope angle on the decision of the dependent variable, i.e., FOS of the rock slope. The correlation matrix, as shown in Table 10, indicates that the independent variables are not correlated to one another. Also, there exists a negative correlation between the width of the weathered layer, MJS orientation, CJS orientation, and slope angle with the FOS, which implies that as the width of the weathered layer, MJS orientation, CJS orientation, and slope angle increases, the FOS of the slope decreases. Also, it can be seen that a minimal positive correlation exists between height and FOS because the bedrock strength governs FOS in high slopes unless there exists a thick weathered rock layer over the bedrock. Table 11 presents the result of the ANOVA analysis. The multiple correlation coefficient indicates that nearly 81% of independent variable correlate with the dependent variable. The adjusted R^2 value indicates that the independent variable accounts for nearly 65.5% variance in the output. The probability value of the F-test is significantly less, which means that the adjusted R^2 is significantly different from zero, which implies that the model as a whole is satisfactorily predicting the FOS. The p-values of the developed model are less than 0.05 for all the independent variables indicating that all the selected independent variables are significantly predicting the dependent variable. The order of reducing the significance of independent variable on the outcome based on correlation matrix and the p-value is weathered layer thickness; slope angle; MJS orientation; slope height; and CJS orientation.

CONCLUSION

Based on the statistical data generated from the field study and laboratory experiments coupled with a detailed literature survey of the study area, probabilistic analysis is performed for stability analysis

under gravity (dry) loading conditions. The following conclusions were drawn based on field investigations and numerical analysis:

- The study area is highly affected by weathering, and anthropogenic activities resulted in the formation of highly fracture surface rock mass. The depth of weathering varies from place to place depending on the local climatic conditions, surface and subsurface hydrology and rampant unplanned anthropogenic activities. The intensity of weathering generally decreases with depth.
- Based on the geological field observations, planar failure has been identified as the primary mode of failure, which can be attributed to the unfavourable orientations of joint sets coupled with steep sloping topography. Field investigation has revealed that the rock mass generally contains numerous discontinuities with different orientations, spacing, persistence and joint characteristics. The valley dipping joint planes are wide open at some places (3cm or even more). During rains, percolation of water along these joint planes led to lowering of shear strength of the rock mass, resulting in failure.
- The orientation of the MJS usually affects the stability of the rock slope. Analysis of results indicates that the maximum yielded elements are around the MJS daylighting in the slope face. A significant reduction in FOS is observed when the MJS dip is in between $\pm 15^0$ of the slope inclination. The orientation of the CJS also affects the FOS of the slope but to a lesser extent.
- FOS of any rock slope having two joint sets decreases in the order of both the joint set orientation differ more than $\pm 15^0$ of the slope inclination; the MJS orientation differ more than $\pm 15^0$ of the slope inclination, but the CJS orientation falls in between $\pm 15^0$ of the slope inclination; the CJS orientation differs more than $\pm 15^0$ of the slope inclination, but the MJS orientation falls in between $\pm 15^0$ of the slope inclination; both the joint set orientation falls in between $\pm 15^0$ of the slope inclination. This order is appropriate for the cases where the failure surface passes through the weathered layer and not for the case where the failure surface passes through the bedrock layer.
- There is a drastic reduction in FOS as the thickness of the weathered layer increases by more than 4m for all slope heights and angles. With the increase in the slope inclination, the variation of FOS for any particular weathered layer thickness reduces, and the slope behaves in an almost similar manner for different joint set orientations except for the case when the MJS and CJS dip in between $\pm 15^0$ of the slope inclination.
- The slopes having greater height have maximum horizontal displacements located near the crest. In contrast, for the slopes with limited height, the maximum horizontal displacement is observed at the toe of the slopes. It was observed that the slopes with a larger number of plastic points have higher stability.
- The effect of orientation of discontinuity sets on decreasing the stability of rock slope is a function of the thickness of the weathered layer. The effect of CJS orientations is prominent in the case of shallow weathered layer and reduces as the thickness of the weathered layer increases. Whereas the effect of MJS orientations is prominent in the case of deep weathered layer and reduces as the thickness of the weathered layer decreases.
- ANOVA analysis indicates that all the independent variables (slope height, weathered layer thickness, MJS orientation, CJS orientation, and slope angle) significantly predict the dependent variable (FOS of rock slope). The reducing order of significance of independent variables on predicting slope stability based on ANOVA and correlation matrix is weathered layer thickness; slope angle; MJS orientation; slope height; and CJS orientation.

References

Abdaqadir, Z.K., Alshkane, Y.M. (2018) Physical and Mechanical Properties of Metamorphic Rocks. Jour. Garmian Univ., v.5, pp.160-173. doi:10.24271/garmian.334

Anbarasu, K., Gupta, S., Sengupta, A. (2009) Site-specific geological and geotechnical studies on the Lanta Khola landslide, North Sikkim Highway, India. Internat. Jour. Geotech. Eng., v.3, pp.361-376 doi:10.3328/IJGE.2009.03.03.361-376

ASTM (2010) D7012 Standard test method for compressive strength and elastic moduli of intact rock core specimens under varying states of stress and temperatures.

ASTM E132 - 04 Standard Test Method for Poisson's Ratio at Room Temperature.

Bachmann, D., Bouissou, S., Chemenda, A. (2004) Influence of weathering and pre-existing large scale fractures on gravitational slope failure: insights from 3-D physical modelling. Natural Hazards: Earth Syst. Sci., v.4, pp.711-717. doi:10.5194/nhess-4-711-2004

Bartarya, S., Valdiya, K. (1989) Landslides and erosion in the catchment of the Gaula River, Kumaun Lesser Himalaya, India. Mountain Res. Develop., v.9, pp.405-419 doi:10.2307/3673588

Barton, N., Bandis, S. (1990) Review of predictive capabilities pf JRC-JCS model in engineering practice. *In:* N. Barton and O. Stephenson (Eds.), Rock Joints. Proc. Int. Symp on Rock Joints, Loen, Norway, pp.603-610

Barton, N., Lien, R., Lunde, J. (1974) Engineering classification of rock masses for the design of tunnel support. Rock Mech., v.6, pp.189-236 doi:10.1007/BF01239496

Brideau, M-A., Yan, M., Stead, D. (2009) The role of tectonic damage and brittle rock fracture in the development of large rock slope failures. Geomorphology, v.103, pp.30-49. doi:10.1016/j.geomorph.2008.04.010

Carter, B.J., Lajtai, E.Z. (1992) Rock slope stability and distributed joint systems. Canadian Geotech. Jour., v.29, pp.53-60 doi:10.1139/t92-006

Chaurasia, A.K., Pandey, H., Nainwal, H., Singh, J., Tiwari, S. (2017) Stability analysis of rock slopes along Gangadarshan, Pauri, Garhwal, Uttarakhand Jour. Geol. Soc. India, v.89, pp.689-696. doi:10.1007/s12594-017-0680-1

Deere, D.U., Miller, R. (1966) Engineering classification and index properties for intact rock vol Tech Report. Air Force Weapons Lab., New Mexico, No. AFNL-TR. Illinois Univ. at Urbana Dept Of Civil Engineering.

Einstein, H., Veneziano, D., Baecher, G., O'Reilly, K. (1983) The effect of discontinuity persistence on rock slope stability. *In:* International journal of rock mechanics and mining sciences & geomechanics abstracts, v.5. Pergamon, pp.227-236. doi:10.1016/0148-9062(83)90003-7

El-Ramly, H., Morgenstern, N., Cruden, D. (2005) Probabilistic assessment of stability of a cut slope in residual soil. Geotechnique, v.55, pp.77-84 doi:10.1680/geot.2005.55.1.77

Ersöz, T., Topal, T. (2018) Assessment of rock slope stability with the effects of weathering and excavation by comparing deterministic methods and slope stability probability classification (SSPC). Environ. Earth Sci., v.77, pp.547 doi:10.1007/s12665-018-7728-4

Fereidooni, D. (2018) Influence of discontinuities and clay minerals in their filling materials on the instability of rock slopes. Geomech. Geoengg., v.13, pp.11-21 doi:10.1080/17486025.2017.1309080

Gerrard, J. (1994) The landslide hazard in the Himalayas: geological control and human action. *In:* Geomorphology and Natural Hazards. Elsevier, pp.221-230. doi:10.1016/B978-0-444-82012-9.50019-0

Ghosh, S., Günther, A., Carranza, E.J.M., van Westen, C.J., Jetten, V.G. (2010) Rock slope instability assessment using spatially distributed structural orientation data in Darjeeling Himalaya (India). Earth Surface Processes and Landforms, v.35, pp.1773-1792. doi:10.1002/esp.2017

Ghosh, S., Kumar, A., Bora, A. (2014) Analyzing the stability of a failing rock slope for suggesting suitable mitigation measure: a case study from the Theng rockslide, Sikkim Himalayas, India. Bull. Engg. Geol. Environ., v.73, pp.931-945 doi:10.1007/s10064-014-0586-8

Gupta, V., Tandon, R.S. (2015) Kinematic rockfall hazard assessment along a transportation corridor in the Upper Alaknanda valley, Garhwal Himalaya, India. Bull. Engg. Geol. Environ., v.74, pp.315-326 doi:10.1007/s10064-014-0623-7

Hencher, S. (1987) The implications of joints and structures for slope stability Slope Stability. John Wiley, Ch 5, pp.145-186.

Israil, M., Pachauri, A. (2003) Geophysical characterization of a landslide site

in the Himalayan foothill region. Jour. Asian Earth Sci., v.22, pp.253-263 doi:10.1016/S1367-9120(03)00063-4

ISRM I (1978) Suggested methods for the quantitative description of discontinuities in rock masses Commission on the standardization of Laboratory and Field Tests in Rock Mechanics, ISRM

ISRM UR, Hudson, J. (2007) The complete ISRM suggested methods for rock characterization, testing and monitoring: 1974–2006 Kozan, Ankara

Jiang, M., Jiang, T., Crosta, G.B., Shi, Z., Chen, H., Zhang, N. (2015) Modeling failure of jointed rock slope with two main joint sets using a novel DEM bond contact model. Engg. Geol., v.193, pp.79-96. doi:10.1016/j.enggeo.2015.04.013

Johari, A., Lari, A.M. (2017) System probabilistic model of rock slope stability considering correlated failure modes. Computers and Geotechnics, v.81, pp.26-38 doi:10.1016/j.compgeo.2016.07.010

Kim, B., Cai, M., Kaiser, P., Yang, H. (2007) Estimation of block sizes for rock masses with non-persistent joints. Rock Mechanics and Rock Engineering, v.40, pp.169 doi:10.1007/s00603-006-0093-8

Kothyari, G.C., Pant, P., Luirei, K. (2012) Landslides and neotectonic activities in the main boundary thrust (MBT) zone: Southeastern Kumaun, Uttarakhand. Jour. Geol. Soc. India, v.80, pp.101-110. doi:10.1007/s12594-012-0123-y

Kumar, R., Anbalagan, R. (2016) Landslide susceptibility mapping using analytical hierarchy process (AHP) in Tehri reservoir rim region, Uttarakhand. Jour. Geol. Soc. India, v.87, pp.271-286. doi:10.1007/s12594-016-0395-8

Kumar, S., Kumar, K., Dogra, N. (2017) Rock mass classification and assessment of stability of critical slopes on national highway-22 in Himachal Pradesh. Jour. Geol. Soc. India, v.89, pp.407-412. doi:10.1007/s12594-017-0622-y

Latha, G.M., Garaga, A. (2010a) Stability analysis of a rock slope in Himalayas. Geomechanics and Engineering, v.2, pp.125-140 doi:10.12989/gae.2010.2.2.125

Latha, G.M., Garaga, A. (2010b) Seismic stability analysis of a Himalayan rock slope. Rock Mech. Rock Engg., v.43, pp.831-843 doi:10.1007/s00603-010-0088-3

Li, Y., Oh, J., Mitra, R., Canbulat, I., Hebblewhite, B. (2019) Applicability of a joint constitutive model: correlation with field observations International Jour. Geotech. Engg., v.13, pp.299-315. doi::10.1080/19386362.2017.1344367

Lie, C., Hack, H. (2015) The effect of discontinuity orientation on the stability of rock masses. *In:* Proceedings of Slope 2015: Advancement of research, practice and integrated solutions on landslides. 27-30 September 2015, Bali, Indonesia.

Little, A. (1969) The engineering classification of residual torpical soils. *In:* Soil Mech & Fdn Eng Conf Proc/Mexico.

Mahanta, B., Singh, H., Singh, P., Kainthola, A., Singh, T. (2016) Stability analysis of potential failure zones along NH-305, India. Natural Hazards, v.83, pp.1341-1357. doi:10.1007/s11069-016-2396-8

Mehrotra, G., Sarkar, S., Kanungo, D., Mahadevaiah, K. (1996) Terrain analysis and spatial assessment of landslide hazards in parts of Sikkim Himalaya Jour. Geol. Soc. India, v.47, pp.491-498.

Pain, A., Kanungo, D., Sarkar, S. (2014) Rock slope stability assessment using finite element based modelling–examples from the Indian Himalayas. Geomechanics and Geoengg., v.9, pp.215-230. doi:10.1080/17486025.2014.883465

Pal, S., Kaynia, A.M., Bhasin, R.K., Paul, D. (2012) Earthquake stability analysis of rock slopes: a case study. Rock Mech. Rock Engg., v.45, pp.205-215. doi:10.1007/s00603-011-0145-6

Park, H-J., West, T.R., Woo, I. (2005) Probabilistic analysis of rock slope stability and random properties of discontinuity parameters, Interstate Highway 40, Western North Carolina, USA. Engg. Geol., v.79, pp.230-250 doi:10.1016/j.enggeo.2005.02.001

Pathak, S., Nilsen, B. (2004) Probabilistic rock slope stability analysis for Himalayan conditions. Bull. Engg. Geol. Environ., v.63, pp.25-32. doi:10.1007/s10064-003-0226-1

Pathak, S., Poudel, R.K., Kansakar, B.R. (2006) Application of Probabilistic Approach in Rock Slope Stability Analysis–Experience from Nepal Disaster Mitig Debris Flows Slope Fail. Landslides, v.2, pp.797-802

Pradhan, S., Vishal, V., Singh, T. (2018) Finite element modelling of landslide prone slopes around Rudraprayag and Agastyamuni in Uttarakhand Himalayan terrain. Natural Hazards, v.94, pp.181-200. doi:10.1007/s11069-018-3381-1

Ray, A., Kumar, R.C., Bharati, A.K., Rai, R., Singh, T. (2019) Hazard Chart for Identification of Potential Landslide Due To the Presence of Residual Soil in the Himalayas. Indian Geotech. Jour., pp.1-16. doi:10.1007/s40098-019-00401-6

Regmi, A.D., Yoshida, K., Dhital, M.R., Pradhan, B. (2014) Weathering and mineralogical variation in gneissic rocks and their effect in Sangrumba Landslide, East Nepal. Environ, Earth Sci., v.71, pp.2711-2727. doi:10.1007/s12665-013-2649-8

Sarkar, K., Singh, A.K., Niyogi, A., Behera, P.K., Verma, A., Singh, T. (2016) The assessment of slope stability along NH-22 in Rampur-Jhakri Area, Himachal Pradesh. Jour. Geol. Soc. India, v.88, pp.387-393 doi:10.1007/s12594-016-0500-z

Shang, J., West, L., Hencher, S., Zhao, Z. (2018) Geological discontinuity persistence: Implications and quantification. Engg. Geol., v.241, pp.41-54. doi:10.1016/j.enggeo.2018.05.010

Shukla, S., Hossain, M. (2011) Analytical expression for factor of safety of an anchored rock slope against plane failure. Internat. Jour. Geotech. Engg., v.5, pp.181-187 doi:10.3328/IJGE.2011.05.02.181-187

Siddique, T., Pradhan, S., Vishal, V., Mondal, M., Singh, T. (2017) Stability assessment of Himalayan road cut slopes along National Highway 58, India. Environ. Earth Sci., v.76, pp.759. doi:10.1007/s12665-017-7091-x

Siddque, T., Pradhan, S. (2018) Stability and sensitivity analysis of Himalayan road cut debris slopes: an investigation along NH-58, India. Natural Hazards, v.93, pp.577-600. doi:10.1007/s11069-018-3317-9

Singh, P., Kainthola, A., Singh, T. (2015) Risk analysis of High Hill Slopes – a case history. Jour. Rock Mech. Tunnel Tech., v.21, pp.101-113

Singh, R., Umrao, R., Singh, T. (2014) Stability evaluation of road-cut slopes in the Lesser Himalaya of Uttarakhand, India: conventional and numerical approaches. Bull. Engg. Geol. Environ., v.73, pp.845-857 doi:10.1007/s10064-013-0532-1

Singh, R., Umrao, R.K., Singh, T. (2017) Hill slope stability analysis using two and three dimensions analysis: A comparative study. Jour. Geol. Soc. India, v.89, pp.295-302 doi:10.1007/s12594-017-0602-2

Starzec, P., Andersson, J. (2002) Probabilistic predictions regarding key blocks using stochastic discrete fracture networks–example from a rock cavern in south-east Sweden. Bull. Engg. Geol. Environ., v.61, pp.363-378. doi:10.1007/s10064-002-0154-5

Stead, D., Wolter, A. (2015) A critical review of rock slope failure mechanisms: The importance of structural geology. Jour. Struc. Geol., v.74, pp.1-23. doi:10.1016/j.jsg.2015.02.002

Umrao, R., Singh, R., Ahmad, M., Singh, T.N. (2011) Stability analysis of cut slopes using continuous slope mass rating and kinematic analysis in Rudraprayag district, Uttarakhand. Geomaterials, v.1. doi:10.4236/gm.2011.13012

Zhang, L., Einstein, H. (2000) Estimating the intensity of rock discontinuities. Internat. Jour. Rock Mech. Mining Sci., v.37, pp.819-837 doi:10.1016/S1365-1609(00)00022-8